Proceedings World Geothermal Congress 2020+1
Reykjavik, Iceland, April - October 2021

Geological Model and Fluid Flow Pathways of the Sol de Mañana/Apacheta Geothermal Field (Altiplano – Bolivia)

Sébastien Haffen (1), Marc Diraison (2), Michel Corsini (3) and Yves Géraud (2)

(1) Teranov SAS, 2 rue du Doyen Marcel Roubault, 54501 Vandœuvre-lès-Nancy, France

(2) GeoRessources lab., UMR 7359, Ecole Nationale Supérieure de Géologie, Université de Lorraine, CNRS, CREGU, 2 rue du Doyen Marcel Roubault, 54501 Vandœuvre-lès-Nancy, France

(3) Université de Nice – Sophia Antipolis, UMR Geoazur, 250 rue A. Einstein, 06560 Valbonne, France

shaffen@teranov.fr

Keywords: Fluid flow pathways, Structural geology, Petrology, Petrophysics, Sol de Mañana, Bolivia

ABSTRACT

Located in the Southwestern part of Bolivia, in the Altiplano area (Andean Mountains), the Sol de Mañana/Apacheta geothermal field, well-known since the 1970's as the Laguna Colorada geothermal project, appears as a target for geothermal development. To that end, it seems important to know as precisely as possible the shape and the properties of the geothermal reservoir components, i.e. local geology and more particularly the structural pattern, the distribution of different lithologies and their associated transfer properties. Indeed, such a knowledge will affect the choice of future drilling sites. For this, the aim of this study is focused on (1) structural analysis: lineaments on DEM, field data and scanline surveys, and (2) matrix characterization: petrological and petrophysical investigations.

The geothermal field is composed of Miocene to Pleistocene volcanic rocks: andesites highlight the well-marked volcanoes and lava flows whereas ignimbrites display a more or less flat topography. At the outcrops-scale, andesites and ignimbrites display evidence of magmatic flow structures, marked in particular by the preferential orientation of minerals, vacuoles and volcanic clasts. Highly hydrothermalized rocks are visible on outcrop, notably close to active fumarolic areas, as in Sol de Mañana, but also in areas without current surface manifestations.

Field and DEM investigations show brittle structures organized according to four main orientations, at different scales: NW/SE, NE/SW, N/S and E/W, leading to an interpreted local compartmentalization of the geothermal reservoir. At the local-scale, a swarm of NW-oriented normal faults with sub-vertical attitude displays a pattern of horsts and grabens system. At the outcrop-scale, numerous non-tectonic brittle structures are also identified and marked by complex curve shapes, with free apertures reaching few centimeters, average extensions of several meters long and with no specific orientation.

Locally, hot fluids circulations caused the formation of secondary mineralogical assemblages corresponding to zeolite-facies conditions. In this case, the mineralogical transformations observed in the rocks show that the fluids have circulated parallel to sub-horizontal magmatic flow structures or along subvertical fracture zones. At depth in the reservoir, higher temperature conditions are confirmed by greenschist-facies mineral assemblages observed in drill core, as well in ignimbrites as in andesites. Such temperature estimate (above 300°C) highly suggests that steep faults evolve at depth into schistose structures which could form more or less horizontal draining zones for the fluids.

Matrix properties are analyzed through petrological and petrophysical studies. Porosity, bulk density, permeability, thermal conductivity and P-wave velocity were measured on andesitic and ignimbritic samples, with two facies: fresh and hydrothermalized rocks.

Structural, petrological and petrophysical data were used to build a 3D geological model of the Sol de Mañana/Apacheta geothermal field. In this new model, structural blocks are limited by main faults whose dips are interpreted to reduce with depth. Convective cells are interpreted to be confined within these separate blocks, resulting in them being a major driver of field geometry and boundaries.

1. INTRODUCTION

In the frame of the worldwide development of geothermal energy, geologists aim to identify fluid flow patterns in rocks and structures forming geothermal reservoirs and in their surroundings. They attempt to identify and propose flow zones and non-flow zones in targeted formations, and characterize their properties (porosity, permeability…), to improve future geothermal reservoirs exploitation/viability. Currently, it is well-known that fluid flows in rocks are supported by either matrix heterogeneities or/and structural components (faults and fractures). Faults are commonly targeted to improve a geothermal plant viability. Nevertheless, matrix heterogeneities have to be studied too, and associated to structural components to better understand fluids distribution inside geothermal reservoirs.

Here, we present the results of a study performed in the area of the Bolivian Sol de Mañana/Apacheta geothermal field (Sud Lipiez Province) (Figure 1), where rocks are mainly ignimbrites and lavas, andesitic to dacitic in composition (Choque, 1996; Lema and Ramos, 1996). This active geothermal field is located about 70 km northwestward of Cerro Zapareli, whose summit is the triple point of the borders of Argentina, Bolivia and Chile, and about 230 km south-southwestward of Uyuni (Potosí Department, Bolivia). It corresponds to one of the more than 70 geothermal manifestations listed in Bolivia (Aliaga, 1984), all are located either in the eastern

slope of the Cordillera Occidental, or in the central part of the Altiplano or in the southern part of the Cordillera occidental (Lahsen et al., 2015).

We present a geological/structural model of the Sol de Mañana/Apacheta geothermal field and of its surrounding, highlighting possible fluid flow pattern: matrix and/or structural support. To build this new model, we studied (1) the structural characteristics of the area of interest: lineaments analysis at different DEM (Digital Elevation Model) scales and fractures orientation at outcrops scale, (2) matrix heterogeneities, notably the lava flow fluidality as a support for fluid flow, and their petrophysical properties (porosity, density, permeability, thermal conductivity and P-wave velocity).

2. FRAMEWORK OF THE STUDY

2.1 Background

Geothermal development started in Bolivia in 1970s and in 1976 began the evaluation of the geothermal potential of the Laguna Colorada project (here called the Sol de Mañana/Apacheta geothermal project). Villarroel Camacho (2014) details the history of the development of the project, summarized hereafter. At the end of the 1980s and early 1990s, 6 wells were drilled (AP-1, SM-1, SM-2, SM-3, SM-4 and SM-5). Temperature and pression logs indicated reservoir condition of 250-260°C and 30-48 bar (Villarroel, 2014). Recently, a project of construction of a 50 MWe geothermal power plant in Sol de Mañana, based on a feasibility studies of 100 MWe, has been studied (West JEC, (2010), mentioned in Villarroel Camacho, (2014)). In 2011, the project's preparatory phase, phase zero, started (see Villarroel Camacho (2014) and Ramos Sullcani (2015) for details).

2.2 Geological setting

The studied area is located SW of Bolivia (Figure 1), at an altitude of about 4900 m.a.s.l. This area is made of Miocene-Pleistocene rocks forming Andes volcanic arc, extending locally more or less in a N/S direction, parallel to the Pacific coast (Ramos Sullcani, 2015). The volcanic arc rocks are of calc-alkaline composition, varying from rhyodacite to andesite, and consisting in lavas, tuff and ignimbrites (Ramos Sullcani, 2015). The regional structures have two main direction: (1) N/S i.e., parallel to the magmatic arc and (2) NW/SE with long alignments along the recent volcanism (see Tibaldi et al. (2009); Tibaldi et al. (2017); Tibaldi and Bonali (2018) for details). So, the volcanism of Laguna Colorada area is part of the Altiplano-Puna Volcanic Complex located in the central Andes (de Sylva et al., 2006; Salisbury et al, 2011). Active since 23 Ma, it is characterized by a large volume of ignimbritic flows and andesitic domes, associated with the formation of numerous calderas, which are controlled by a NW-SE fault system (Acocella, 2014).

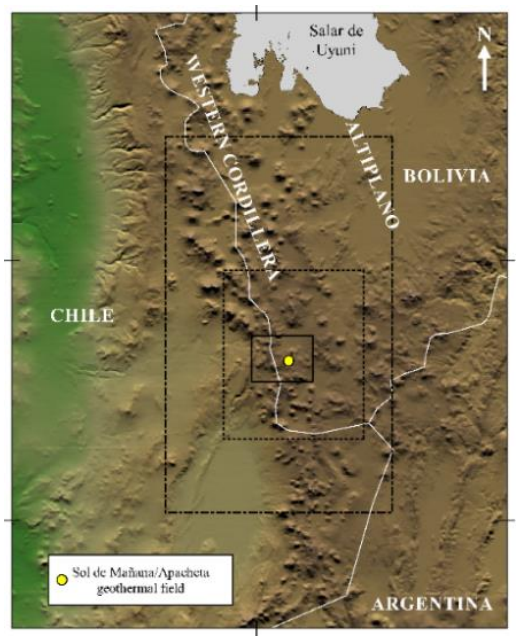

Figure 1: Location of the Sol de Mañana/Apacheta geothermal field in the Bolivian central Andean Altiplano (topographic map: GTOPO30 DEM). The black continuous line rectangle, the black dotted rectangle and the black point-dash rectangle localize areas where lineaments study were undertaken at different scale, respectively 1:100,000, 1:400,000 and 1:1,000,000.

The local mapping (Choque, 1996; Lema and Ramos, 1996) indicates the existence of extensive ignimbritic sequences that cover an important part of the area, overlying andesitic-dacitic lava sequences and possible ignimbrites from Neogene. The associated structural geology (Choque, 1996; Lema and Ramos, 1996; Tibaldi et al., 2009; JICA, 2015; Tibaldi and Bonali, 2018) displays two more or less orthogonal tectonic systems, oriented NNW/SSE and NNE/SSW respectively. The first system is more marked and affects the most recent formations, notably by the formation of small horsts and grabens. The structural organization caused secondary deep fracturing, allowing hot water to rise up. Part of the geothermal fluid rises as vapor through fractures and faults to reach the surface in springs, resulting in hydrothermal alteration zones (CFE, 1997, mentioned by Ramos Sullcani, (2015)).

3. METHODOLOGY

3.1 Lineaments analysis

The lineament analysis of the area of interest was based on extraction of lineaments from DEM interpretation in a GIS (Geographic Information System) tool. The used 3D topographic surfaces representations were computed from SRTM1 (Shuttle Radar Topography Mission) data set, with about 30 m resolution. To illuminated/shaded the surface, differential lighting angles were modeled with the aim to avoid overestimation of perpendicular lineaments compared with parallel lines generated by the lighting. Lineaments were manually highlighted thanks to each shaded map. Lineaments were considered as linear of slightly curvilinear structural unit (O'Leary et al., 1976), their lengths and azimuths (or mean azimuths calculated between the two extremities in the case of curvilinear unit) were extracted to be characterized. The plot cover area at different scale: 1:1,000,000, 1:400,000 and 1:100,000, and was combined into a single plot to give a multiscale point of view.

3.2 Petrophysical technics

Porosity, density, permeability, thermal conductivity and P-wave velocity of rocks from selected outcrops were measured thanks to classic laboratory methods (see Haffen, 2012 for detailed methodology description). Samples were analyzed either under dry condition (air saturated) or under wet condition (water saturated). Samples are in dry condition after having been dried to a constant weight in a heat chamber at 50°C. The wet condition is reached by submerging samples in distilled water inside a sealed vacuum chamber for 48h (inspired by the standard NF P 94-410-3 (AFNOR, 2001): first, samples were placed in a first high-vacuum chamber, during 24h, whereas distilled water is placed in a second vacuum chamber, then samples were progressively submerged in distilled water, and finally samples stayed in distilled water, during at least 24h.

4. STRUCTURAL CHARACTERITICS

4.1 Lineament maps

4.1.1 1:1,000,000 scale

From the analysis of the DEM data set at a scale of 1:1,000,000 (Figure 2a), 247 lineaments are highlighted, presenting a mean length of 6.788 km. The average lineament density of the whole map reaches 0.0049 lineaments/km². Note that the relative low density is notably induced by the presence of several areas without lineaments corresponding to flat salars, lagunas, Quaternary undifferentiated deposits … (see for example Tibladi et al. (2009)). The diagram of lineaments orientations (Figure 2d), regrouped in 10° bins, highlight two main lineaments families: N010°-N040°E, about 37.7% of the lineament total length, and N150°-N160°E, about 13.3% of the lineament total length. Two secondary families are also depicted: N080°-N100°E and N110°-N150°E, about 10.7 and 19.1% of the total length respectively.

The NNE trend lineaments are organized according three main clusters of more than 50 km long and 20 km large in the whole map. The southernmost cluster starts from the lower left corner of the map whereas the northernmost one stops from the upper right corner of the map, in the prolongation of the previous one. The third cluster, presents an eastward shift in the middle of the map. The SSE trend lineaments appear more regularly spaced from the upper left corner to the lower right corner of the map. The other two families are more randomly distributed in the whole map. The length distribution of the lineaments plotted in Figure 3 exposes a power low distribution outside the sampling biases. This power law has and exponent a = -4.752 and is valid for lineaments length approximatively between 8,500 and 20,1000 m.

4.1.2 1:400,000 scale

The DEM study performed at 1:400,00 scale (Figure 2b) depicts 236 lineaments presenting a mean length of 4.638 km and a whole density of 0.0167 lineaments/km². As in the previous case, the quite low density of lineament can be partially explained by the presence of current Salar and Lagunas in the investigated area. The diagram of lineaments orientations (Figure 2d) shows two main lineaments families: the first includes lineaments oriented N020°-N040°E, about 32.6% of the total length, whereas the second is mainly orientated N120°-N130°E, about 11.8% of the total length. Note that for this last family, the length repartition in function of the orientation suggest a more or less Gaussian distribution, centered on N120°-N130°E and with a large range from N080°E to N180°E.

The N120°-N130°E trend is well marked between the NW and the SW of the map, with a high concentration of lineaments close to the Sol de Mañana/Apacheta geothermal field. The NNE trend present a clustered pattern from the lower left corner of the map to the Laguna Colorada. This cluster seems to continue in the NNE direction after a shift eastward of about 20 km. The length distribution of lineaments (Figure 3) shows a power law distribution, outside of the sampling biases, and has an exponent a = -3.974 and is valid for lineaments length raging from about 6,500 to 10,500 m.

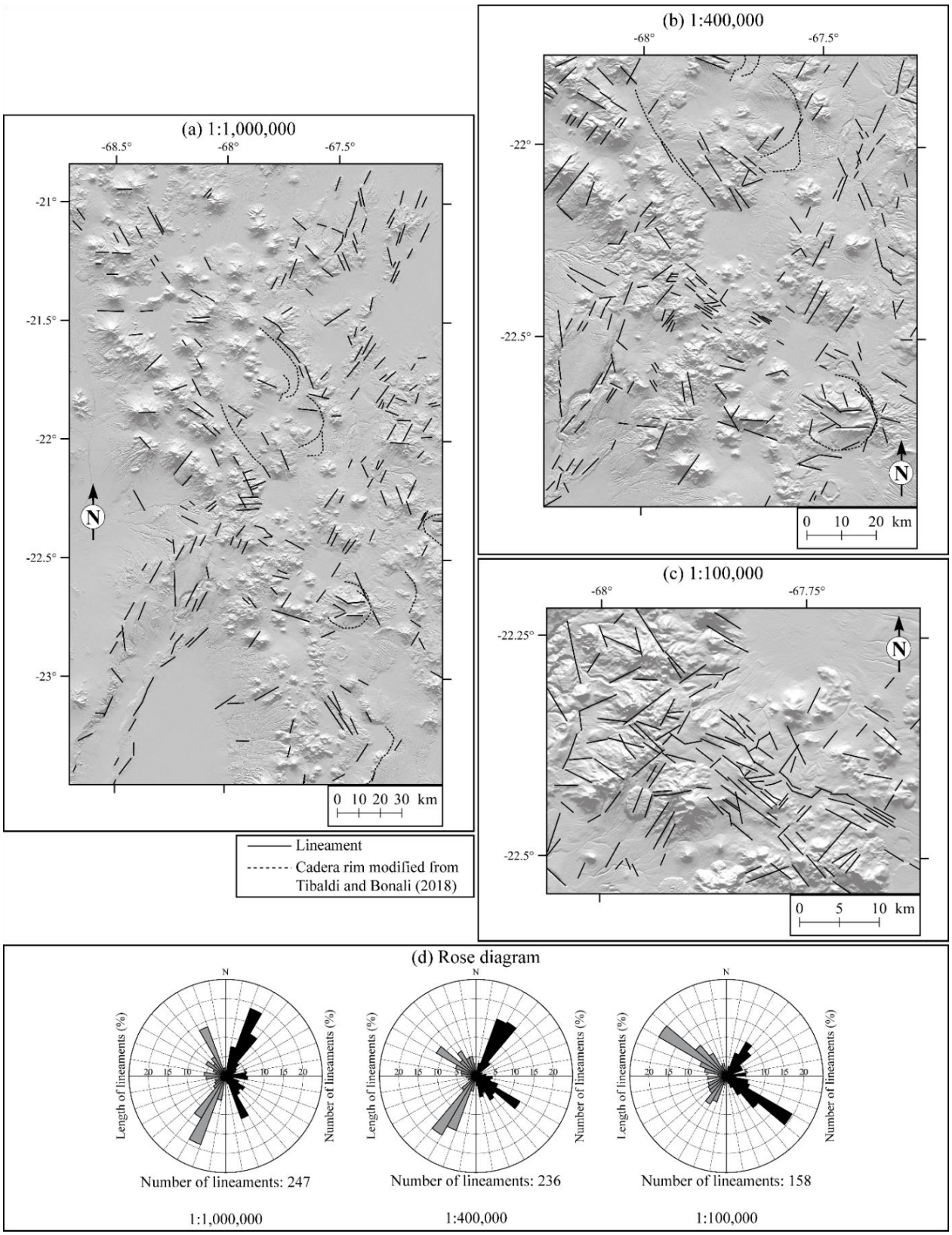

Figure 2: (a) Lineament traces analysis performed at the 1:1,000,000 scale (see text for DEM details), (b) lineament traces analysis performed at the 1:400,000 scale, (c) lineament traces analysis performed at the 1:100,000 scale, (d) associated lineament number/length orientation rose diagram.

4.1.3 1:100,000 scale

The structural analysis performed at the 1:100,000 scale (Figure 2c) presents 158 lineaments: the mean length is 3.014 km and the whole density reaches 0.0930 lineaments/km². The repartition of the lineament distribution in the whole map is quite homogeneous, expected in the NE where the Laguna Colorada prevents observations. The diagram of lineament orientation (Figure 2d) depicted one main orientation: N110°-N140°E which represent 37.9% of the total length. Two secondary lineaments families are observable and oriented N020°-N050°E and N080°-N090°E, corresponding respectively to 21.3 and 4.8% of the total length.

The main family correspond to a swarm of lineament, about 30 km long and 15 km large, centered on the Sol de Mañana/Apacheta geothermal field and corresponding to the Sol de Mañana Graben. The length distribution of lineaments (Figure 3) shows a power law distribution, outside of the sampling biases, with an exponent a = -3.569 valid for lineament length ranging from about 3,100 to 9,000 m.

4.1.4 Multiscale length distribution

In order to compare the different scale of observations (Pickering et al., 1995), the cumulative length distribution for each map/scale were plotted together, normalized by the surface area of each map (Figure 3). Over the studied data range, the power law segment of each map can be linked to the others by a mean power law on lineaments extended from about 3,100 to 20,100 m in length, presenting an exponent a = -3.768 (Figure 3). That mean that the lineaments length distribution can be mathematically simplified as a power law valid for the explored scales. As the power law is sufficiently clear at the studied scales, tests could be attempted to explore the validity of this power law at higher scales.

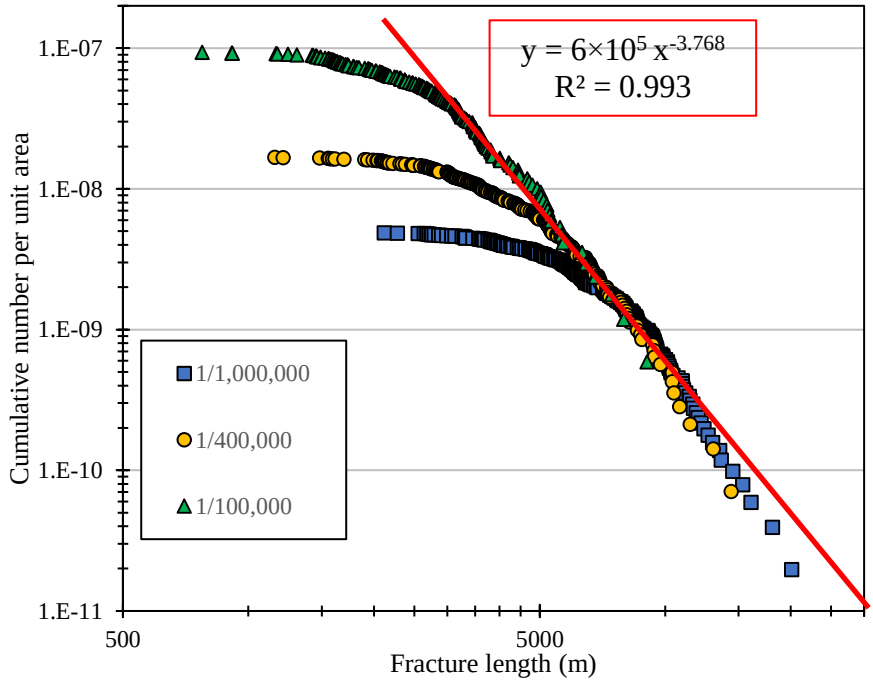

Figure 3: Lineament length distribution of the studied area at different scales (1/1,000,000, 1/400,000 and 1/100,000), each plot corresponding to the entire data set. The correlation line has been fitted to the different data set manually.

4.2 Structural map

We propose a new structural map (Figure 4) of the Sol de Mañana/Apacheta Geothermal Field. This map was built in taking into account structural data from previous studies and direct field observations performed during this study. Structural data were extracted from Choque et al. (1996), JICA (2015), Tibaldi et al. (2009) and, Tibaldi and Bonali (2018). Lineaments (1:100,000 scale, Figure 2c) were too added to build the structural map. Also, we propose to modify some structures suggested by previous authors, notably in elongating them thanks to satellite imagery and DEM observations. Finally, we added five faults observed directly in the field and/or inferred from DEM/satellite imagery performed at high scale (>1:100,000).

The structural map (Figure 4) highlight the NW/SE oriented, 25 km long, Sol de Mañana Graben. Fault relative density appears more important inside and close to the graben than in its surroundings. Faults forming the shoulders of the graben appears divided in several segments with variable length (from about 2.5 to 10 km long), with locally relay zone in between. Both meridional and septentrional shoulders of the graben are marked by a system of more or less parallel, conjugated (?) or antithetic/synthetic (?) faults, about 1 km apart, forming locally tilted (?) blocs, horsts or graben. The main central graben is marked by several structures trending E/W to SW/NE, locally affecting too the graben shoulders. In the surroundings of the graben, tectonic structures are oriented either with a trend parallel of the graben or with a NW/SE trend.

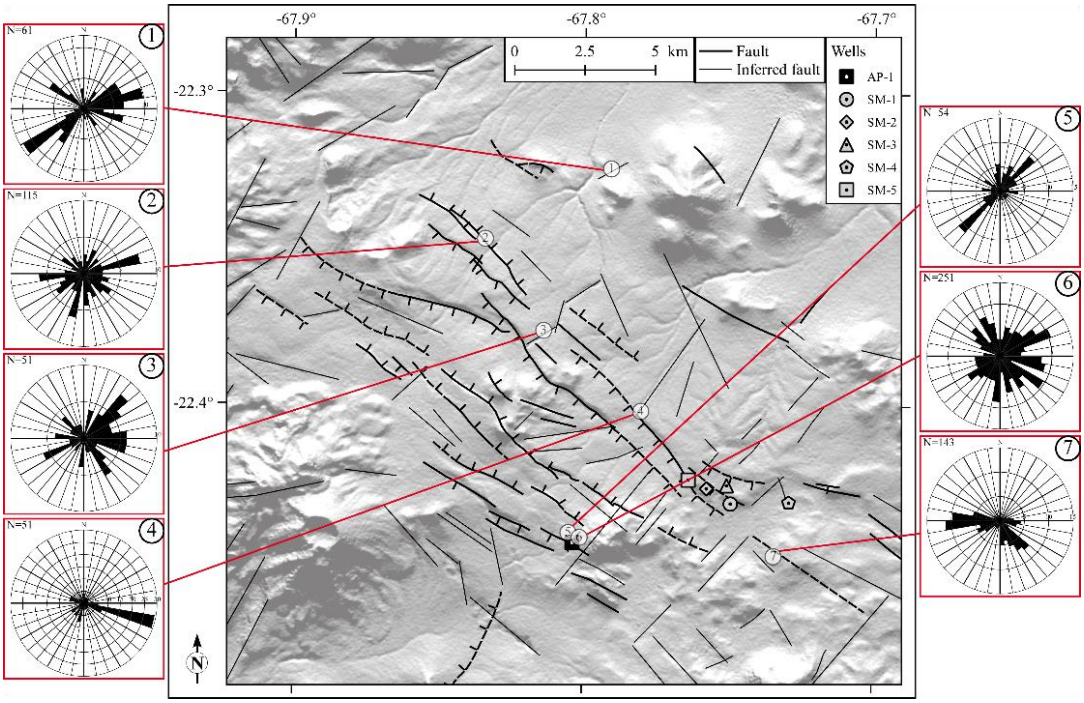

Figure 4: Structural map of the Sol de Mañana/Apacheta geothermal field. Data are modified from Choque (1996), Tibaldi et al. (2009), JICA (2015), Tibaldi and Bonali (2018), lineament analysis performed in this study at 1:100,000 scale (Figure 2c) and are from field observations performed during this study (topographic map: SRTM1 DEM). Rose diagrams (1, 2, 3, 4, 5, 6 and 7) depict fractures orientations measured directly on outcrops, the location of the selected outcrops is indicated in the map by the rose diagrams references respectively.

4.3 Fractures orientations: outcrop scale analysis

Fractures, from decimetric to decametric scale, were characterized thanks to systematic measurement of the orientations of fractures along scanlines on seven selected outcrops located inside and on the shoulders of the Sol de Mañana graben. The statistical orientation of fractures is displayed in rose diagrams given in Figure 4.

Structural analysis performed through fractures orientations characterization in several outcrops, located in different structural context across the Sol de Mañana Graben, point out that outcrop scale fractures are organized according to four main orientations. A first group shows fractures that are oriented either with a NW/SE trend, i.e., parallel to the graben orientation, or with a SW/NE trend, i.e., perpendicular to the graben trend and parallel to many inferred faults. These structures orientations were also well described in lineament analysis and so they appear to be of first order. A second group displays fractures oriented either N/S or E/W. These orientations were poorly depicted in the lineament analysis, and so these fractures appear to be of second order.

4.4 Sol de Mañana/Apacheta geothermal field

4.4.1 Surface and wells data

Thanks to the new structural map (Figure 4) and with the help of the geological map of the area of interest drawn by Choque (1996)(Figure 5), we propose a new geological/structural cross section, oriented WSW/ENE, intersecting both Apacheta and Sol de Mañana area. JICA (2015) provided a basic lithological description with the main geological unities (not associated with surface lithological description done by Choque (1996)) intersected by the wells of Apacheta and Sol de Mañana sites. This data was also used to build the cross section (Figure 5) and notably the description of andesite lava at depth, both in Apacheta and Sol de Mañana, which could be correlated (JICA, 2015).

4.4.2 Structural and geological pattern

The cross section through the Apacheta/Sol de Mañana geothermal field displays two main structure: (1) the horst of Apacheta and (2) the graben of Sol de Mañana. The well of Apacheta (AP-1) is located close to the meridional fault of the Apacheta horst. The septentrional fault of the horst marks also the meridional fault of the graben. Note that recent deposits forming Cerro Apacheta prevent to see possible associated faults that would exist below and not activated since these deposit emplacements. The septentrional shoulder of the graben is made of three blocks, bordered by four faults. The two faults located the most SW correspond to major faults forming the graben border, several kilometers long (about 8 and 10 km long respectively) and trending from Sol de Mañana to the NW. The other two faults are no more than 3 km long and are only located in the Sol de Mañana area. Most of the wells of Sol de Mañana (SM-1, SM2, SM-3 and SM-5) are located precisely in between these four faults.

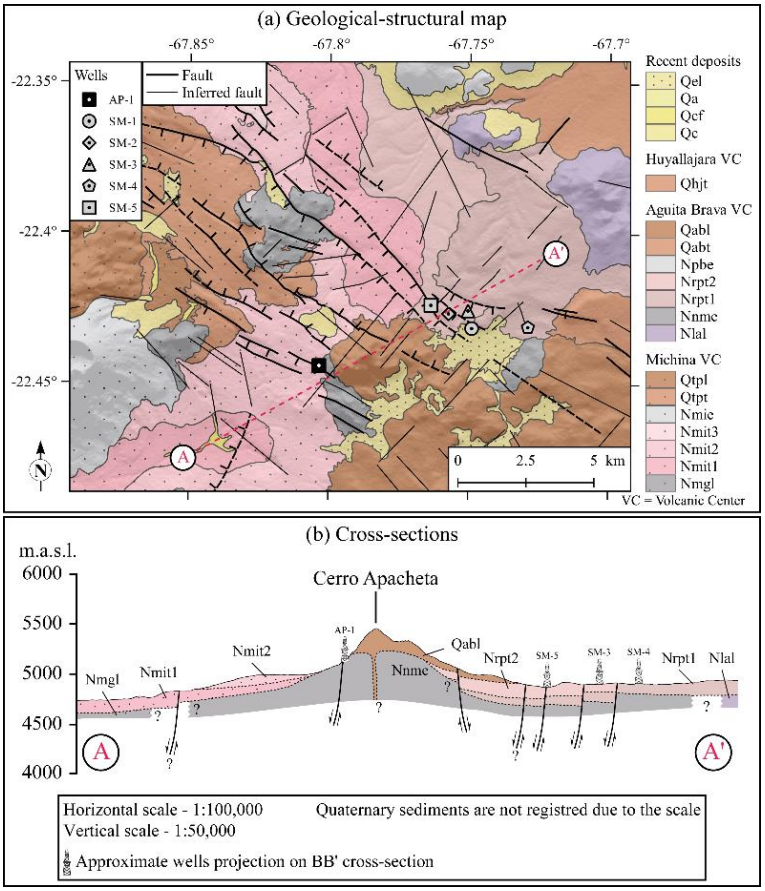

Figure 5: (a) Geological-structural map of the surroundings of the Sol de Mañana/Apacheta geothermal field. Lithologies are modified from Choque (1996), structural data are given in Figure 4. The red dotted lines (AA') locate cross-sections given in (b).

5. MATRIX CHARACTERITICS

At the outcrop-scale, the ignimbritic flows are massive and display typical cooling structures characterized by metric-scale subvertical columns (Figure 6a). They contain a large number of volcanic enclaves (pumice, andesite, dacite, rhyolite), among which pumice enclaves present a highly flattened shape Figure 6c, d and e). The magmatic fluidality is underlined by subhorizontal planes (Figure 6b) corresponding to the alignment of feldspar and amphiboles phenocrysts and by flattened pumice enclaves.

At thin section-scale, the ignimbrites exhibit a microlithic texture with fine plagioclase rods and phenocrystals of feldspar and amphiboles floating in an amorphous glass. Depending of their quartz content, the ignimbrites have a rhyolitic to dacitic character.

Locally ductile deformation is marked by the appearance of sub-vertical schistosity (Figure 6f). These ductile deformation corridors are marked by a concentration of hydrothermal circulation with significant petrographic and structural transformation.

At thin section-scale, this metamorphic transformation is expressed by the formation of reaction crowns between feldspars and zeolites, which are preferentially carried out in privileged hydrothermal fluid circulation planes. In the most hydrothermalized rocks, mineralogical transformations are very advanced and results in the formation of clays. Fluids circulation is confirmed by the concentration of metamorphic minerals in veins parallel to the magmatic fluidity (Figure 7a). Hence, the initial magmatic plane of the lava flows constitutes a privileged drain for fluid circulation. When the fluid circulations stop, the rock cools down and the drains are sealed by late metamorphic crystallizations.

The conditions of alteration at depth can be estimated using cores extracted from the boreholes. In the deepest levels, at about 1700 m depth, the rocks present a very intense hydrothermal alteration state. Under the microscope, the primary mineralogical (Figure 7b) consists of Quartz + Feldspar + Micas + Amphiboles corresponding to an andesite. This mineralogy is transformed by hydrothermal metamorphism into a secondary mineralogical assemblage with Quartz + Sericite + Epidote + Actinote + Chlorite + Prehnite + Sphene. This paragenesis corresponds to the "Sub-Greenschist" facies for temperature conditions such as 250°C < T < 320°C. The distribution of the mineralogical assemblages observed between the surface and the bottom of the wells confirms the increase in temperature, associated with the presence of a deep heat source.

(a)

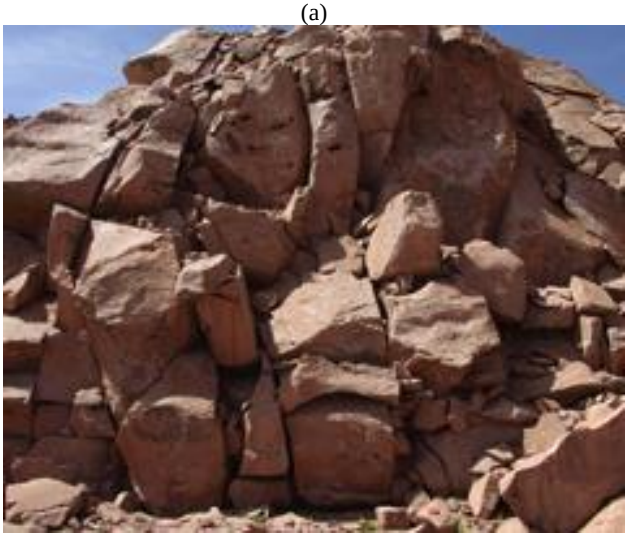

(b)

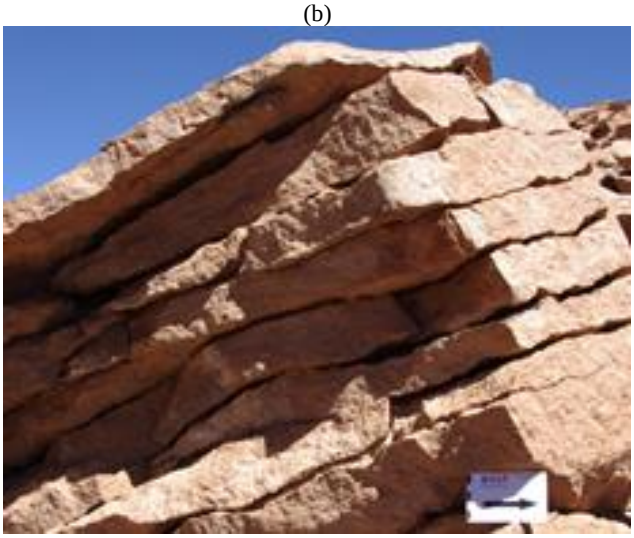

(c)

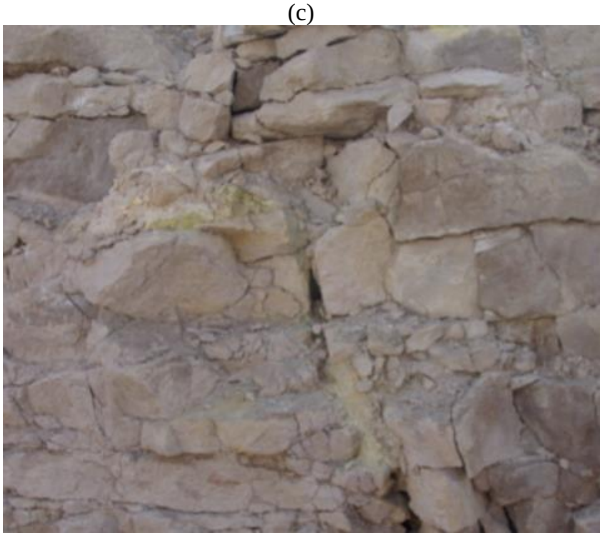

(d)

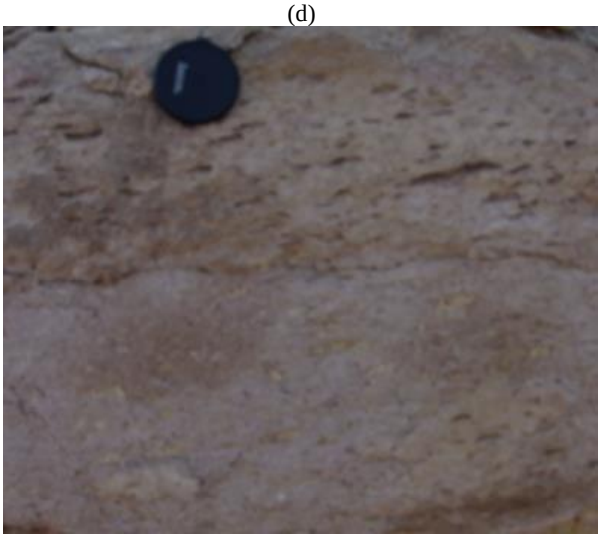

(e)

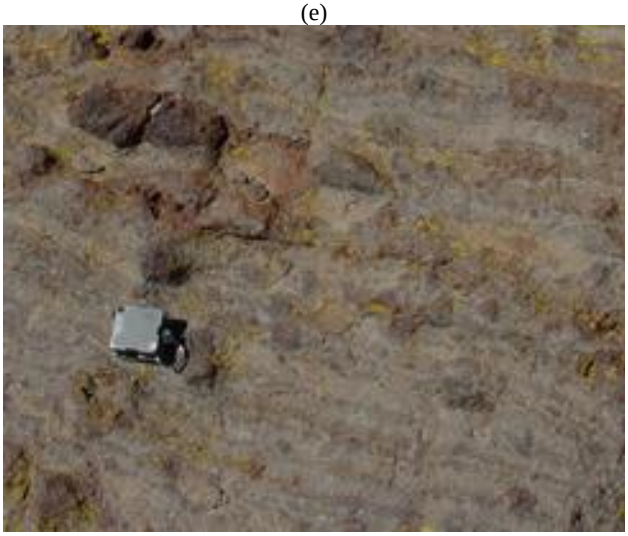

(f)

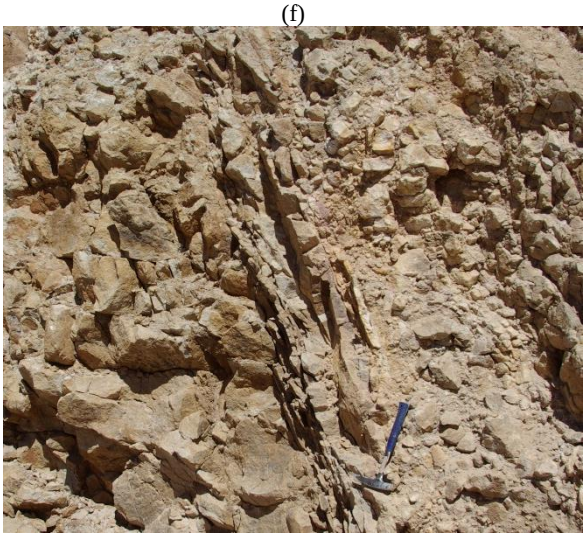

Figure 6: Photography of ignimbritic flow at the outcrop-scale. (a) subvertical columns, (b) subhorizontal planes, (c) subvertical fractures cutting the subhorizontal flow planes underlined by sulfur deposits, (d) magmatic flow highlighted by pumice enclaves, (e) magmatic flow highlighted by pumice enclaves, (f) ductile deformation corridor

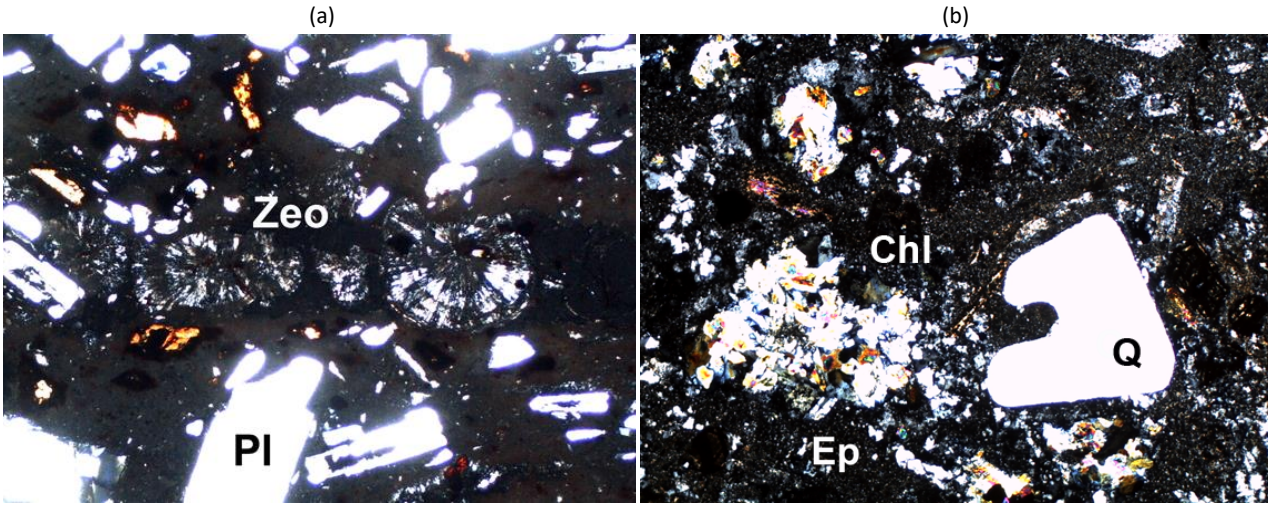

Figure 7: Microphotographs from hydrothermalized volcanic rocks (LPA), (a) ignimbrite from Apacheta, (b) ignimbrite from Borehole SM-5 (Chl: Chlorite, Ep: Epidote, Q: Quartz, Pl: Plagioclase, Zeo: Zeolite)

6. PETROPHYSICAL CHARACTERITICS

Measured petrophysical characteristics aim to provide a data set to help the interpretation of seismic profiles and well data, and to allow future modelling of fluid flow in the reservoir.

Fresh andesitic and ignimbritic rocks present the following properties respectively (11Figure 8): porosities range from 5.61 to 9.24% and from 13.74 to 18.40%, whereas bulk densities display values from 2.19 to 2.29 $g.cm^{-3}$ and from 2.09 to 2.23 $g.cm^{-3}$. Permeabilities show values from 7.78 to 2322.06 mD and from 18.25 to 143.93 mD, dry thermal conductivities vary from 1.00 to 1.26 $W.m^{-1}.K^{-1}$ and from 0.91 to 1.24 $W.m^{-1}.K^{-1}$, whereas wet thermal conductivity are from 1.45 to 1.86 $W.m^{-1}.K^{-1}$ and from 1.56 to 1.82 $W.m^{-1}.K^{-1}$. Dry P-wave velocities display values from 1040 to 2787 m/s and from 1892 to 3301 m/s, whereas wet P-wave velocities range from 2992 to 4334 m/s and from 2143 to 3694 m/s. Hydrothermalized andesitic and ignimbritic rocks present the following properties respectively (Figure 8): porosities range from 4.03 to 12.05% and from 6.39 to 20.46%, whereas bulk densities display values from 1.99 to 2.47 $g.cm^{-3}$ and from 1.84 to 2.62 $g.cm^{-3}$. Permeabilities show values from 0.01 to 9.10 mD and from 0.01 to 74.38 mD, dry thermal conductivities vary from 1.01 to 2.54 $W.m^{-1}.K^{-1}$ and from 0.80 to 2.71 $W.m^{-1}.K^{-1}$, whereas wet thermal conductivity are from 1.38 to 2.76 $W.m^{-1}.K^{-1}$ and from 1.46 to 2.98 $W.m^{-1}.K^{-1}$. Dry P-wave velocities display values from 1475 to 4077 m/s and from 976 to 4739 m/s, whereas wet P-wave velocities range from 2738 to 4608 m/s and from 2211 to 5301 m/s.

Porosities measured in andesitic samples are globally less important than those measured in ignimbritic ones (Figure 8). Relation between measured bulk density and porosity (Figure 8a) suggests the occurrence of a petrologic family presenting a skeleton density of about 2.6. Some hydrothermalized facies display less important measured bulk densities than expected for equivalent porosities. Two possibilities can be presented to explain this characteristic: (1) their petrology is strongly different, and/or (2) they present alteration of primary minerals.

Lava samples with low measured permeabilities (Figure 8b) show no or very few cracks, whereas those with cracks display high permeabilities values. Ignimbritic samples show globally more important permeability values, nevertheless in some samples, alteration process drives to decrease the permeability.

At first order, thermal conductivity and P-wave velocity measured on water and air saturated samples (Figure 8c, d, e, f) are controlled by the porosity of rocks. Nevertheless, rock texture, voids shapes and cracks can strongly modify the thermal conductivity and P-wave velocity in some facies.

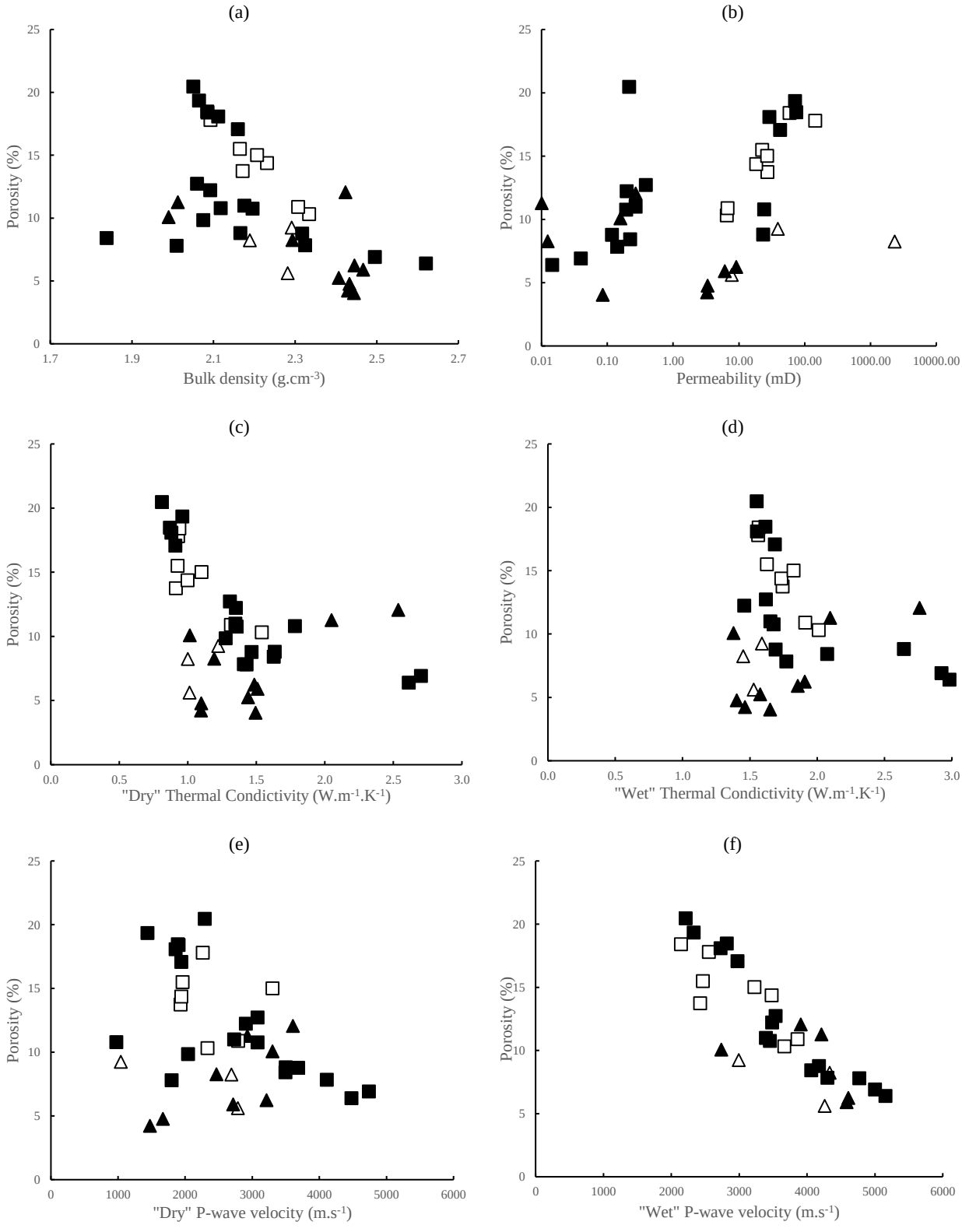
(a)
Porosity (%)
Bulk density (g.cm-3)
(b)
Porosity (%)
Permeability (mD)
(c)
Porosity (%)
"Dry" Thermal Condictivity (W.m-1.K-1)
(d)
Porosity (%)
"Wet" Thermal Condictivity (W.m-1.K-1)
(e)
Porosity (%)
"Dry" P-wave velocity (m.s-1)
(f)
Porosity (%)
"Wet" P-wave velocity (m.s-1)

Figure 8: Petrophysical characteristics of fresh and hydrothermalized andesite (white and black triangle respectively) and fresh and hydrothermalized ignimbrite (white and back square respectively)

7. NEW GEOLOGICAL/STRUCTURAL MODEL

Figure 9 displays a 3D geological/structural model, pointing out all the information about the possible supporting components (matrix and structural) of fluid flow in the studied reservoir. We argue that, in the case of the horst of Apacheta and the graben of Sol de Mañana, faults are the main component for vertical fluid flow. Nevertheless, magma fluidality can be transformed and used as a horizontal pathway for fluid transfer.

Also, we propose to include in this model the position of the brittle ductile transition at depth thanks notably to a model proposed by Favier et al. (in prep.). Faults observed at the surface, most often strongly dipping, must be rooted on the brittle-ductile transition, and potentially tend to be more or less horizontal at that depth. This interface could be potentially interpreted as a preferential pathway for regional heat and fluid transfers, in connection to the already known faults network or matrix heterogeneities.

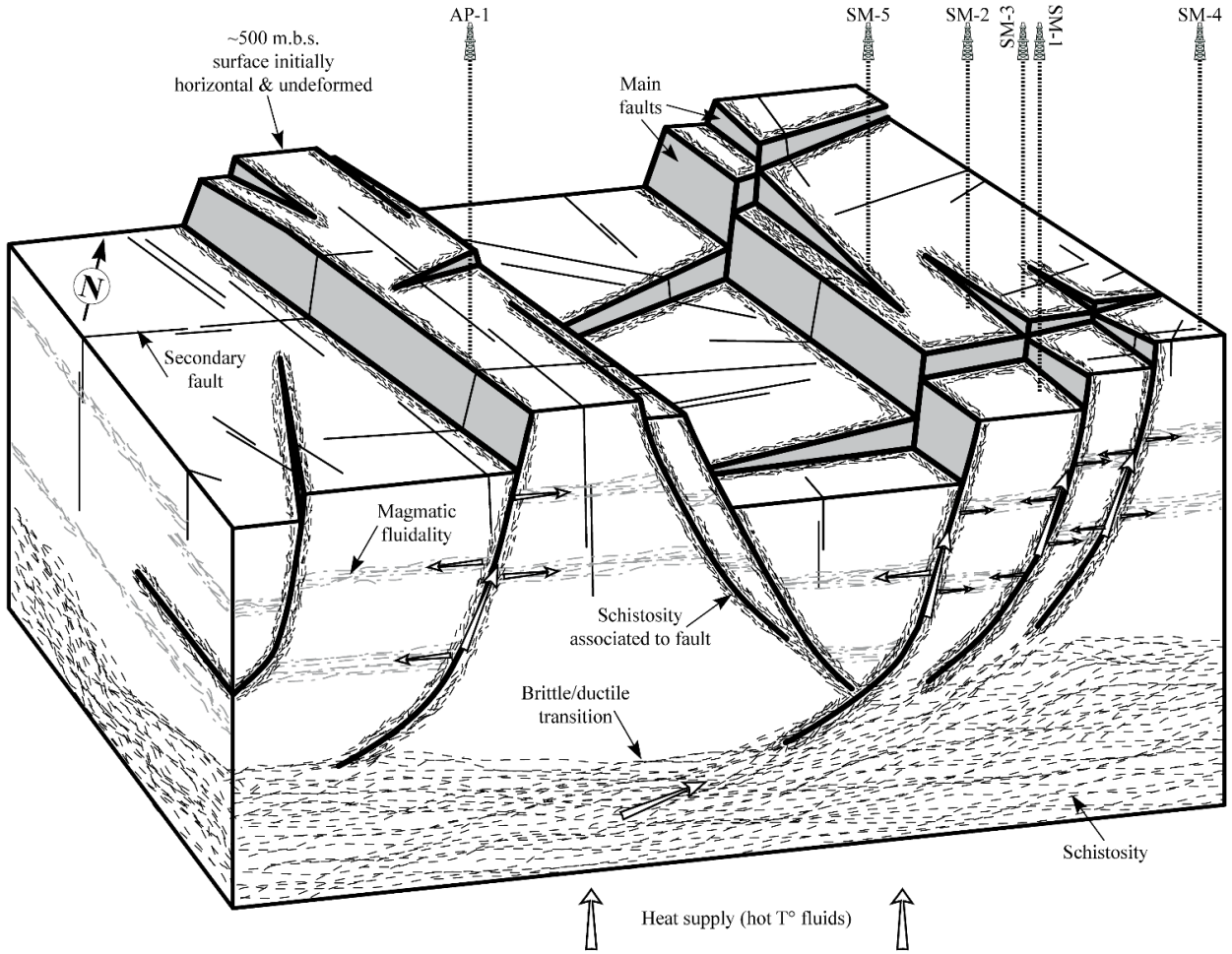

Figure 9: 3D structural bloc (not to scale) of the Sol de Mañana/Apacheta geothermal field. The upper surface of the bloc consists in an arbitrary initially horizontal surface, locates about 500 m.b.s., allowing to highlight current main and secondary tectonic structures at depth. The relative positions of wells are indicated until the upper horizontal surface of the bloc. The biggest and the smallest white arrows indicate possible hot fluid flow in fault zones and in magmatic fluidality respectively.

8. CONCLUSION

In this paper, we present some of the results of a new geological/structural study performed in the area of the Sol de Manana geothermal target. DEM and field investigation drive us to propose a new structural model of the Sol de Manana/Apacheta system,

highlighting two main structural directions, i.e., parallel and perpendicular to the Sol de Manana graben, and two secondary structural directions, i.e., with N/S and E/W direction.

All the data drive us to the building of a new 3D geological/structural bloc model. This model displays main fault organization in the area of interest, and suggest local horizontal flowing zone supported by matrix heterogeneities. This result opens new perspectives for exploration of geothermal resources already known and exploited in the Sol de Manana graben.

REFERENCES

Acocella, V.: Structural control on magmatism along divergent and convergent plate boundaries: Overview, model, problems. *Earth-Science Reviews* **136,** (2014), 226-288.

AFNOR: Roches – Essais pour déterminer les propriétés physiques des roches. Partie 3 – Détermination de la porosité, (2001).

Aliaga, R. C.: Geothermal potential in Bolivia. In *Proc*. 6th NZ Geothermal Workshop, (1984).

CFE: Potential certification of Sol de Mañana geothermal field. Comisión Federal de Electricidad (CFE), internal report submitted to ENDE (in Spanish), (1997), 225 pp.

Choque, N.M.: Hoja Volcán Putana 6026. *Carta Geológica de Bolivia*, Escala 1: 100000, Publicación SGM Serie I-CGB-41, Servicio Nacional de Geología y Minería de Bolivia, (1996).

De Silva, S., Zandt, G., Trumbull, R., Viramonte, J. G., Salas, G., and Jiménez, N.: Large ignimbrite eruptions and volcano-tectonic depressions in the Central Andes: a thermomechanical perspective. *Geological society*, London, special publications **269**.1, (2006), 47-63.

Favier, A., Lardeaux, J.M., Legendre, L., Verati, C., Philippon, M., Corsini, M., Münch, P., and Ventalon, S. : Tectono-metamorphic evolution of shallow crustal levels within active volcanic arc. Insights from exhumed Basal Complex of Basse-Terre (Guadeloupe, French West Indies). *In prep*.

Haffen, S. : Caractéristiques géothermiques du réservoir gréseux du Buntsandstein d'Alsace. Thèse, Université de Strasbourg, (2012).

JICA: Asistencia especial para la implementación del proyecto (SAPI) para el proyecto de construcción de la planta geotérmica Laguna Colorada (fase 1 de la primera etapa), Informe Final, (2015).

Lahsen, A., Rojas, J., Morata, D., & Aravena, D.: Exploration for high-temperature geothermal resources in the Andean countries of South America. In *Proceedings* World Geothermal Congress, (2015), pp. 19-25.

Lema, J.C.Z. and Ramos, W.C.: Hoja Silala-Sanabria 5927-6027. *Carta Geológica de Bolivia*, Escala 1: 100000, Publicación SGM Serie I-CGB-43, Servicio Nacional de Geología y Minería de Bolivia, (1996).

O'leary, D. W., Friedman, J. D., and Pohn, H. A.: Lineament, linear, lineation: some proposed new standards for old terms. *Geological Society of America Bulletin*, **87**(10), (1976), 1463-1469.

Pickering, G., Bull, J. M., and Sanderson, D. J.: Sampling power-law distributions. *Tectonophysics*, **248**(1-2), (1995), 1-20.

Ramos Sullcani, P.R.:. Well data analysis and volumetric assessment of the Sol de Manana geothermal field, Bolivia. United Nation University, *Geothermal Training Programme*, (2015), Number 30.

Salisbury, M. J., Jicha, B. R., de Silva, S. L., Singer, B. S., Jiménez, N. C., and Ort, M. H.: 40Ar/39Ar chronostratigraphy of Altiplano-Puna volcanic complex ignimbrites reveals the development of a major magmatic province. *Geological Society of America Bulletin* **123**.5-6, (2011), 821-840.

Tibaldi, A., Corazzato, C., and Rovida, A.: Miocene–Quaternary structural evolution of the Uyuni–Atacama region, Andes of Chile and Bolivia. *Tectonophysics*, **471**(1-2), (2009), 114-135.

Tibaldi, A., Bonali, F. L., and Corazzato, C.: Structural control on volcanoes and magma paths from local-to orogen-scale: The central Andes case. *Tectonophysics*, **699**, (2017), 16-41.

Tibaldi, A., and Bonali, F. L.: Contemporary recent extension and compression in the central Andes. *Journal of Structural Geology*, **107**, (2018), 73-92.

Villarroel Camacho, D. G.: Geochemical studies of geothermal fluid and evaluation of well test results from wells SM-01, SM-02 and SM-03, Sol de Mañana field, geothermal project, Laguna Colorada, Bolivia. United Nation University, *Geothermal Training Programme*, (2014), Number 32.

Villarroel, D.: Geothermal development in Bolivia. Presented at *"Short Course on Utilization of Low- and Medium-Enthalpy Geothermal Resources and Financial Aspects of Utilization*", organized by UNU-GTP and LaGeo, Santa Tecla, El Salvador, (2014), 6 pp.

West JEC: Preparatory study for the geothermal development of Sol de Mañana, Bolivia. West JEC, internal report (in Spanish), submitted to ENDE, Bolivia (2010).